Available online at www.sciencedirect.com

SCIENCE DIRECT®

Remote Sensing of Environment 96 (2005) 509 – 517

Remote Sensing of Environment

www.elsevier.com/locate/rse

Discrimination of hoary cress and determination of its detection limits via hyperspectral image processing and accuracy assessment techniques

Jacob T. Mundt[a,*], Nancy F. Glenn[a], Keith T. Weber[b], Timothy S. Prather[c], Lawrence W. Lass[c], Jeffrey Pettingill[d]

[a]*Idaho State University-Boise Center, 12301 W Explorer Drive, Suite 102, Boise, ID 83713, United States*
[b]*Idaho State University GIS Training and Research Centre, Campus Box 8130 Pocatello Idaho 83209-8130*
[c]*University of Idaho, United States*
[d]*Bonneville County Weed Control, United States*

Received 21 September 2004; received in revised form 31 March 2005; accepted 2 April 2005

Abstract

This study documents successful discrimination of hoary cress (*Cardaria draba*) in southwestern Idaho using hyperspectral imagery to a maximum producer's accuracy of 82% for infestations with greater than 30% cover. Different hyperspectral processing parameters were evaluated and compared, including data transformations, endmember selection, classification algorithms, and post-classification accuracy assessment methods. In this study, the Spectral Angle Mapper (SAM) and Mixture Tuned Matched Filtering (MTMF) classification algorithms performed equally. Minimum Noise Fraction (MNF) data transformation generated producer's accuracies 23% higher than did similar classifications using Principal Components Analysis (PCA) transformed data. Two hoary cress endmembers derived from different vegetative regimes were necessary for successful classification. Finally, this study documents a methodology comparing incremental map accuracies to optimize classifier performance and determine the detectable limits of hoary cress. Detection limits using hyperspectral imagery were as low as 10% cover over a 3 m × 3 m pixel using a mesic vegetative regime endmember. However, for management level use of the imagery, both a mesic and a xeric endmember were necessary for the 30% cover threshold.

Keywords: Hoary cress; Spectral Angle Mapper; Mixture Tuned Matched Filtering

1. Introduction

Hoary cress (*Cardaria draba*) is an invasive plant that is listed as a noxious weed in the State of Idaho (Prather et al., 2002). It is a 1–2 ft tall rhizomatous perennial that thrives in disturbed semiarid landscapes. During bloom, hoary cress exhibits dense white flowers that give the plant a flat and mat-like appearance. Management of hoary cress is moderately difficult, often requiring the use of herbicides. The weed spreads rapidly via anthropogenic and wildlife vectors, and as a result land managers have the need to understand its distribution to aid in management decisions.

The objectives of this study are: (1) to map the distribution of hoary cress using hyperspectral imagery acquired over a study area in southwestern Idaho, and (2) to evaluate and compare different hyperspectral analysis parameters for hoary cress discrimination. This study was completed under a NASA sponsored initiative to bring science and technology applications into an operational context. The methods and discussion presented herein are intended to serve as guide for hyperspectral image processing techniques for vegetative species discrimination.

The study area (−111°20′W, 43°30′N) is located in relatively flat terrain that is heavily utilized for agriculture in Ada County, Idaho (Fig. 1). Ten-mile Creek, several ditches and canals, and a well-developed network of roads provide transport vectors for hoary cress, which forms infestations diverse in both size (contiguous hectares to smaller than 10

* Corresponding author. Tel.: +1 208 685 6769.
E-mail address: mundjaco@isu.edu (J.T. Mundt).

0034-4257/$ - see front matter © 2005 Elsevier Inc. All rights reserved.
doi:10.1016/j.rse.2005.04.004

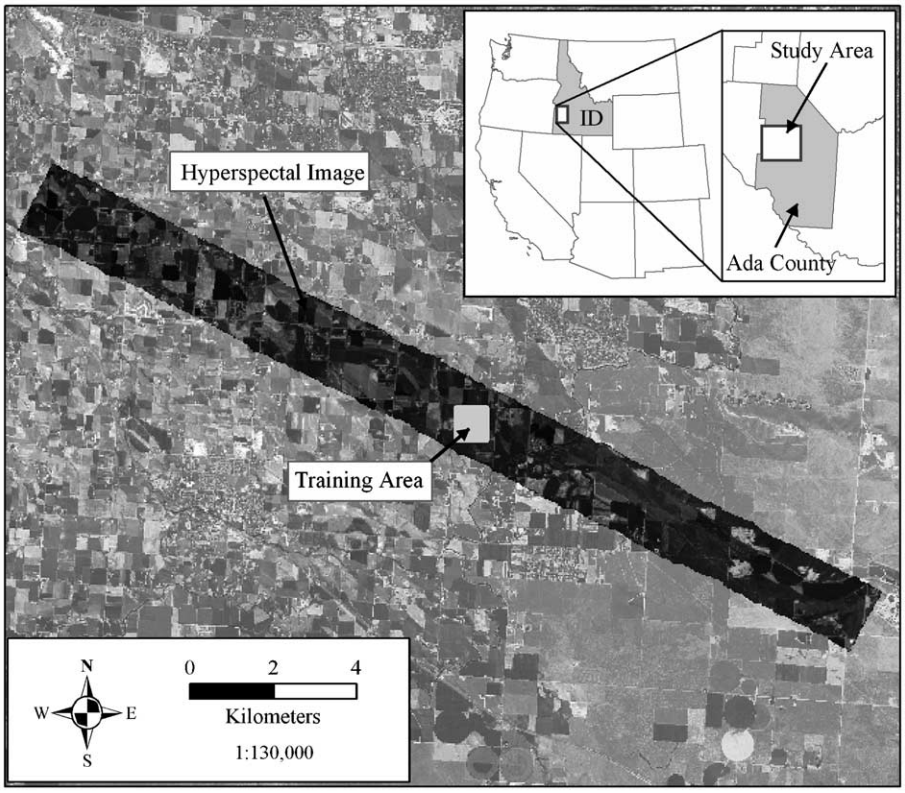

Fig. 1. Location of the study area in Ada County in southwest Idaho. Illustrated training area is enlarged in Fig. 2.

m^2) and percent canopy cover (herein referred to as 'percent cover' or 'cover'). Vegetation in the study area is locally variable, including mesic (e.g. bluegrass (*Poa* spp.) and orchardgrass (*Dactylis glomerata* L.)), and xeric (e.g. cheatgrass (*Bromus tectorum* L.), blue mustard (*Chorispora tenella* (Pall.) D.C.) and wild rose (*Rosa multiflora* Thunb. ex Murr)) vegetative regimes. Typically, infestations of hoary cress with high cover (~100%) are correlated with mesic regimes, while xeric regimes host smaller infestations with lower cover (~60% to 80%).

2. Previous work and technical background

Because different vegetation types have different spectral characteristics (Everitt et al., 2001; Gates et al., 1965; Kondrat'yev & Fedchenko, 1981), many studies have utilized remote sensing techniques to generate distribution maps for invasive species rather than relying solely on the use of a field crew (e.g. Everitt et al., 1995; Glenn et al., 2005; Parker-Williams & Hunt, 2002). In general, studies using multispectral data for species distribution mapping have found limited success, while some have demonstrated encouraging results (e.g. Everitt et al., 1995; Everitt & Yang, 2004; Lass & Callihan, 1997). Previous studies utilizing hyperspectral remote sensing data, however, have demonstrated successful discrimination of invasive species such as leafy spurge (*Euphorbia esula*) and iceplant (*Carpobrotus edulis*) (Glenn et al., 2005; Parker-Williams & Hunt, 2002; Underwood et al., 2003). The study presented herein builds upon this previous work by applying similar hyperspectral processing techniques to hoary cress, and by providing a comparison between different image processing parameters for vegetative species discrimination.

Hyperspectral data analysis can be described in three phases: Pre-processing (atmospheric and geometric correction), processing (endmember selection, data transformation, and classification), and post-processing (accuracy assessment and map interpretation). In this study we compare the following three hyperspectral data analysis parameters: (1) Principal Components Analysis (PCA; Lillesand & Kiefer, 2000) versus Minimum Noise Fraction (MNF; Green et al., 1988) data transformations, (2) Mesic versus xeric hoary cress classification endmembers, and (3) Mixture Tuned Matched Filtering (MTMF; Boardman, 1998) versus Spectral Angle Mapper (SAM; Kruse et al., 1993) classification algorithms. Additionally, incremental classification accuracies are used as an interpretative tool to evaluate classifier performance and determine the minimum percent cover necessary for target detection.

Because hyperspectral datasets are large (> 1 GB) they are commonly transformed to reduce spectral redundancy and emphasize the importance of unique reflectance features. Transformations decorrelate and compact spectral

information into fewer bands with decreasing data coherence (Lillesand & Kiefer, 2000). PCA is a linear solution of reflectance data projected on rotated orthogonal axes in *n*-dimensional space (Davis, 1986; Lillesand & Kiefer, 2000). The MNF transform can be described as a two phase PCA, first projecting mean corrected noise whitened data into its respective eigenvector space, and secondly performing a standard principal components transform on the resulting decorrelated matrix (Green et al., 1988). MNF transforms have been documented to be more consistent in the arrangement of data by band coherence than PCA rotations (Green et al., 1988).

Transformed hyperspectral data is often classified using SAM or MTMF algorithms. SAM calculates a vector angle in *n*-dimensional space between a reference spectra and each pixel in the image. A smaller spectral angle represents a similar spectral profile and a higher likelihood that the pixel contains the target (Kruse et al., 1993). Because classifications are made on the basis of a vector angle, the SAM classifier is insensitive to changes in surface albedo and does not estimate target abundance (Lillesand & Kiefer, 2000). Alternatively, MTMF is a partial unmixing algorithm that is capable of determining target abundance within a pixel (Boardman, 1998). MTMF first projects MNF input data onto the training data vector to determine the spectral component of the target in each pixel (Matched Filter (MF) value), and the noise variance in the MNF data is subsequently used to calculate a value of infeasibility for each pixel (Boardman, 1998). Pixels containing a target component will have both a MF value greater than zero and a low value of infeasibility.

3. Methods

3.1. Data collection

Hyperspectral data was acquired by the HyMap sensor (operated by HyVista, Inc.) over the study area (1.75 by 22 km; 3 m spatial resolution) on May 21, 2003, while hoary cress was blooming (Fig. 1). The hyperspectral sensor collected 126 contiguous spectral bands representing the intensity of reflected solar radiation between the wavelengths of 450 nm and 2500 nm, with radiometric resolutions of ~15 nm (Kruse et al., 2000). Concurrent with image acquisition in 2003, Global Positioning System (GPS) polygons representing locations of hoary cress absence and presence (with oblique estimations of cover) were recorded. The GPS data were collected using Trimble GeoXT model GPS receivers (Trimble, Sunnyvale CA) and were differentially corrected. A total of 209 GPS validation polygons were collected in the 2003 and 2004 field seasons (97 presence and 28 absence in 2003, and 64 presence and 20 absence in 2004). Field validation in both years occurred while hoary cress was blooming, and because the infestations in the study area are typically very well established, little change was assumed between years.

3.2. Pre-processing

Data used in this study were atmospherically corrected using the Fast Line-of-sight Atmospheric Analysis of Spectral Hypercubes (FLAASH) algorithm. FLAASH calculates values of apparent reflectance based on MODTRAN code, accommodates for pixel adjacency errors, and spectrally polishes output values (RSI, 2001). Following atmospheric correction, the data were examined for spectral quality, and bands 63 (1391 nm), 64 (1491 nm), and 126 (2492 nm) were removed due to decreased data coherence from water absorption.

A significant georegistration error is illustrated in Fig. 2, where classified pixels are morphologically similar yet offset from GPS validation polygons. To assess the magnitude of this error, 41 GPS ground control points were collected and used to calculate a Root Mean Square Error (RMSE) of 25 m in non-uniform directions. Because the RMSE is in non-uniform directions, it was not possible to shift the data to accommodate the error. Another common approach to reducing geometric error is to rectify the image to GPS ground control points. Due to atmospheric turbulence during correction, however, the error was locally variable (Fig. 2), and polynomial resampling did not improve the errors. Some related studies document that buffering validation samples may accommodate this error (Glenn et al., 2005; Parker-Williams & Hunt, 2004). However, in this study, the mean georegistration error exceeded the distance separating some GPS validation polygons, resulting in overlapping validation sample buffers. This confused accuracy assessment, and therefore buffering was not a plausible solution. No alternative method was identified, and as a result, classifications and accuracy assessments did not accommodate this error.

3.3. Processing

Data reduction transformations were applied to the datasets using the 123 reflectance bands (having previously removed 3 spectral bands). Rotated or transformed data (such as MNF or PCA) is characterized by high data variance in the first few bands with decreasing data variance in the later bands, where the last bands are noise dominated. To optimize image processing, it is common to process only those bands comprising the dominant (coherent) variance; however, it has not been quantified how this selection should be made. For this study, the first 80% of the cumulative transformed band variance (the first 39 bands) was assumed to represent the coherent variance in the data. The 80% threshold was chosen because it corresponded closely to the flattening of the MNF eigenvalue plot and a complete loss in visible data

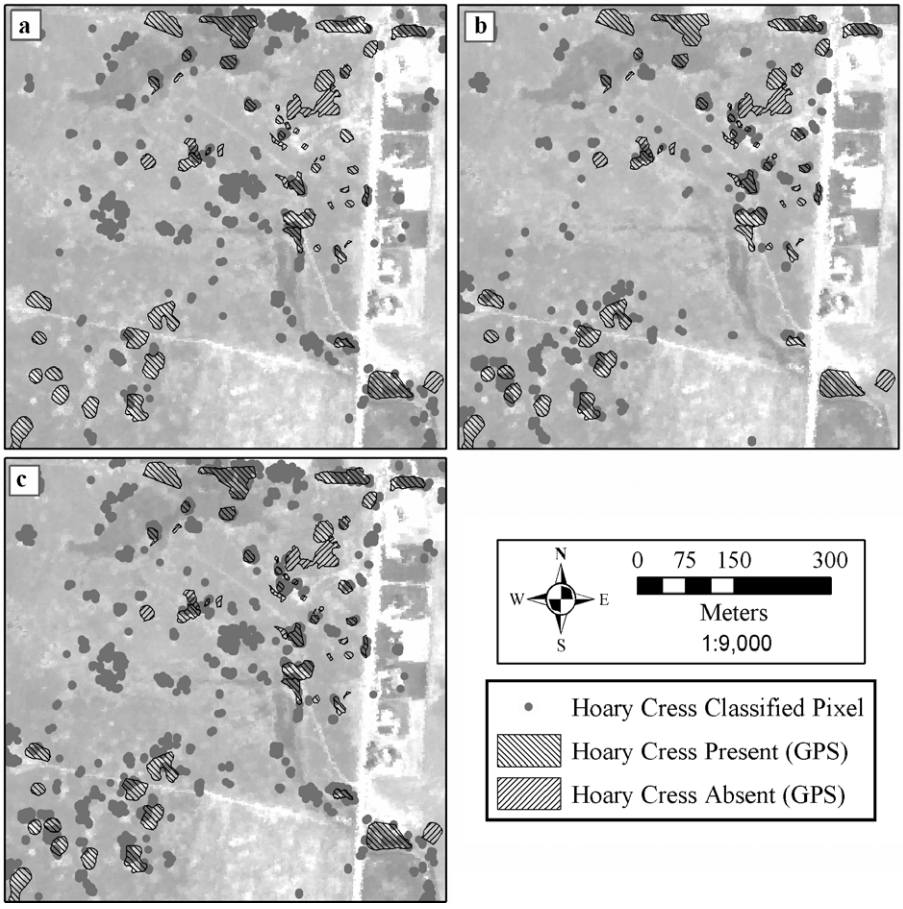

Fig. 2. SAM classification of hoary cress from the training area (see Fig. 1) using: (a) only the mesic endmember, (b) only the xeric endmember, and (c) the combination of the mesic and the xeric endmembers. Numerous satellite infestations illustrate the geometric imprecision of the imagery, where clusters of classified pixels fall just outside of GPS polygons.

coherence. The number of bands to use was determined by solving Eq. (1) for N:

$$\frac{\sum_{i=1}^{N}\sigma}{\sum_{i=1}^{123}\sigma} = 0.8 \quad (1)$$

where i=the number of bands, σ=the band variance, and N=the number of bands comprising 80% cumulative variance.

Supervised image classification (such as SAM and MTMF) requires the input of training endmember pixels. Discussions of training endmember selection have been introduced in peer reviewed literature (Chen & Stow, 2002; Okin et al., 1998; Roberts et al., 1998), but further discussion of target variability is necessary to understand the repercussions of endmember selection. In this study, large infestations of hoary cress with high percent cover are visible in the imagery (Fig. 2), which was used as a processing advantage in endmember selection. Fifty samples (pixels) from high cover patches of hoary cress were manually selected as regions of interest from both the mesic and xeric vegetative regimes, and an arithmetic mean of the selected regions was used to calculate the spectral endmembers used for classification. In general, the mesic endmember demonstrated higher reflectance in the near infrared and higher absorption in the shortwave infrared as compared to the xeric endmember (Fig. 3). The differences between endmembers are hypothesized to be due to variability in: (1) total leaf area, (2) leaf moisture, (3) understory vegetative composition, and (4) soil spectral components (e.g. Knipling, 1970).

This study tested the impacts of different classification parameters by assessing relative changes in classification accuracy. To minimize error propagation, relative accuracies were determined by holding two of three classification parameters (data transformation, training endmember input, or classification algorithm) constant while varying the third parameter. SAM classification accuracies were calculated at different threshold angles and the highest accuracy was used to represent the optimal classification, which was subsequently used for comparison. A parallel approach was used for MTMF classifications. While there may be small deviations in accuracy with small changes in classification thresholds, these biases were minor compared to differences resulting from variations in classification methods.

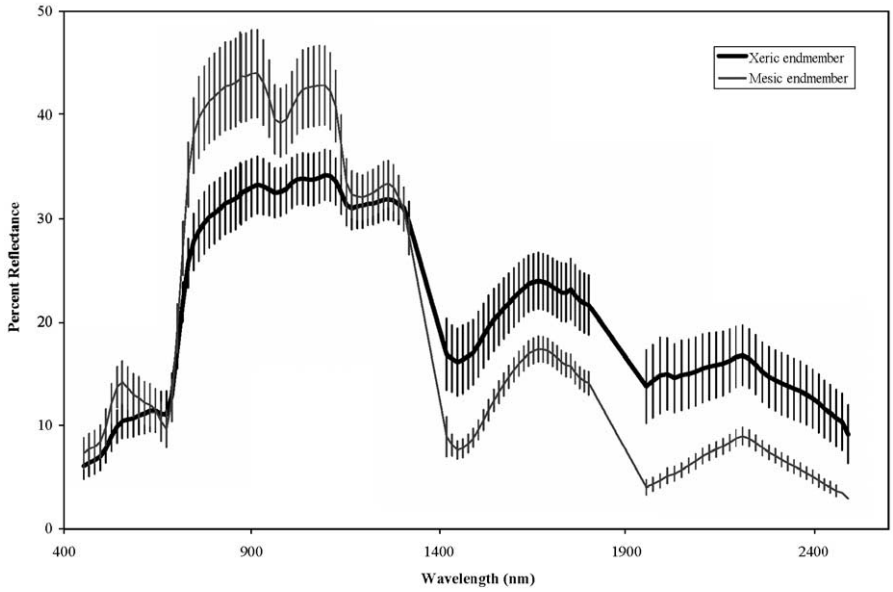

Fig. 3. Hoary cress endmember spectra from mesic and xeric ecological zones, derived from a 50-sample mean. Error bars represent one standard deviation of variance in each profile, and demonstrate spectral separability of the two endmembers.

To test the effect of changing data transformation methods, SAM classifications resulting from both MNF and PCA transformed data were compared for the mesic hoary cress endmember. The variance of the PCA transformed data was more skewed than in the MNF transform, with the first band containing 96% of cumulative variance. For consistency, the first 39 bands of the PCA transform were used in further processing (same number of bands comprising 80% of the cumulative FLAASH MNF variance). A SAM threshold of 1 radian was optimal for the MNF transformed data, while a threshold of 0.45 radians was the optimal threshold for the PCA transformed data.

Because both the PCA rotation and the MNF transform seek to maximize spectral variance, rule images resulting from SAM classifications in transformed space have consistently higher angles (for all pixels) as compared to their reflectance-derived angle equivalents. Further, MNF inversion (transforming the noise-whitened matrix back into reflectance space) generally produces much smaller spectral angles than those derived in transformed space. In this study the distribution of hoary cress was more effectively predicted by SAM classifications in transformed space than it was by the same classifications in reflectance space.

To address the use of different classification strategies for discrimination of hoary cress, the previously derived MNF transformed SAM classification was compared to a MTMF classification generated using the same classification endmember. Using geographically large areas of known hoary cress presence, expected values of MF and infeasibility were determined to be greater than zero and less than 15, respectively.

Selection of classification endmembers from either the xeric or mesic regime could impact classification results because the classifier may exclude occurrences based on the spectral influence of the host regime (e.g. Okin et al., 1998). SAM classifications resulting from both the mesic (developed in the previous comparison) and the xeric endmembers (SAM threshold of 0.75 radians) were compared. Endmember classifications were assessed both individually and by combining the classifications from each endmember to form a single classification.

3.4. Post-processing

Two of the most important components in the interpretation of a classified image are field validation and accuracy assessment (Stehman, 1992). This study builds on previous discussions of accuracy assessments for remote sensing classifications (Congalton, 1991; Foody, 2002; Parker-

Table 1
Example of an error matrix used to generate tabulated accuracies for Table 2

		Reference		Column totals	User's accuracy	
		Present	Absent			
Classified	Present	35	6	41	85%	
	Absent	15	42	57	74%	
Row totals		50	48	98		
Producer's accuracy		70%	88%		Overall accuracy	78%
Total positives		50			Kappa	0.57
Total negatives		48			*Z*-statistic	6.92

This example uses the SAM classification of the MNF transformed data for the combined endmembers with hoary cress polygons greater than 10% cover (SAM/MNF/C).

Table 2
Comparison of classification accuracies resulting from different image processing parameters

Classification	Polygons containing hoary cress	Polygons not containing hoary cress	Producer's accuracy	User's accuracy	Overall accuracy	Kappa statistic	*Z*-statistic
SAM/PCA/M	161	48	31%	96%	46%	0.15	1.47
SAM/MNF/M	161	48	54%	96%	63%	0.30	3.88
MTMF/MNF/M	161	48	57%	94%	64%	0.30	3.88
SAM/MNF/X	161	48	30%	94%	45%	0.13	1.25
SAM/MNF/C	161	48	65%	95%	70%	0.38	5.35
SAM/MNF/M (greater than 10% cover)	50	48	46%	85%	68%	0.57	6.92
SAM/MNF/M (greater than 20% cover)	41	48	54%	85%	74%	0.61	7.25
SAM/MNF/M (greater than 30% cover)	28	48	64%	82%	82%	0.69	8.06
SAM/MNF/C (greater than 10% cover)	50	48	70%	85%	78%	0.57	6.92
SAM/MNF/C (greater than 20% cover)	41	48	73%	83%	81%	0.61	7.25
SAM/MNF/C (greater than 30% cover)	28	48	82%	79%	86%	0.69	8.06

SAM=Spectral Angle Mapper classification; MTMF=Mixture Tuned Matched Filter classification; MNF=Minimum Noise Fraction transform; PCA=Principal Components Analysis transform; M=Mesic hoary cress endmember; X=Xeric hoary cress endmember; C=Combined Mesic and Xeric hoary cress endmember. The classification methods are expressed in the format 'Classification Algorithm'/'Transform'/'Endmember'.

Williams & Hunt, 2004; Stehman & Czaplewski, 1998; Story & Congalton, 1986). Error matrices were generated to assess true positive, false positive, false negative, and true negative occurrences as described by Congalton and Green (1999). Table 1 provides an example of such an error matrix. Accuracies were evaluated and compared using significance testing at two levels: (1) the significance of independent values of Kappa (*Z*-test) and, (2) the differentiability of two values of Kappa (*t*-test) (Congalton & Green, 1999; Foody, 2004). A *Z*-statistic exceeding its respective critical value indicates that the classified Kappa statistic is representative of the data, and a *t*-statistic (*t*-stat) exceeding its critical value indicates that two classifications are significantly different from one another (Davis, 1986).

This study assumes that pixels containing low percent cover hoary cress (or any target) will not classify as accurately as high percent cover pixels (e.g. convex mixing; Boardman, 1998). It follows that the producer's accuracy of a classification should increase with percent target cover. Based on this relationship, an Incremental Cover Evaluation (ICE) analysis, (evaluating changes in producer's accuracy at cumulative 10% increments of target cover) was used as an interpretation of classifier performance. ICE analysis was utilized to quantify the quality of the classifications, and to determine the minimum percent cover of hoary cress necessary for detection. Because user's accuracy is linearly dependent on producer's accuracy when the number of negative reference validation samples is fixed (e.g. in the same classification), ICE methodology need only be applied to the producer's accuracy.

If ICE determines that producer's accuracies increase to acceptable levels at reasonable percent target cover (determinations made at project level), it is inferred that the classification method is performing acceptably. In the event that ICE does not determine acceptable producer's accuracies for reasonable percent target cover, it is concluded that processing methods are not optimal, and the classification strategy should be modified. If iterative classification and ICE assessment fails to determine acceptable producer's accuracies, it should be considered that the detection limit of the target has been met, or that the chosen classification strategy is not capable of discriminating the target.

4. Results and discussion

4.1. Processing

Data reduction transformations demonstrated large accuracy differences when classifying with SAM using the mesic endmember. The PCA classification resulted in producer's, user's, and overall accuracies of 31%, 96%, and 46%, respectively (Table 2; SAM/PCA/M). The same classification applied to the MNF transformed data generated producer's, user's, and overall accuracies of 54%, 96%, and 63%, respectively (Table 2; SAM/MNF/M). While significance testing between the respective Kappa values produced a non-significant *t*-stat of 1.19 (Table 3), visual evaluation of the classification indicated that the MNF transformed classification outperformed the PCA transformed classification. Thus, the MNF transformed data was used for the remainder of the study.

Table 3
Test statistics (*t*-stat) resulting from comparison between processing parameters

Classification 1 (Kappa value)	Classification 2 (Kappa value)	*t*-stat
PCA (0.15)	MNF (0.30)	1.19[a]
MTMF mesic (0.30)	SAM mesic (0.30)	0.03[a]
SAM xeric (0.13)	SAM combined (0.38)	1.97[a]
SAM mesic (0.30)	SAM mesic ICE 10% (0.57)	0.43[b]
SAM mesic (0.30)	SAM mesic ICE 20% (0.61)	0.15[b]
SAM mesic (0.30)	SAM mesic ICE 30% (0.69)	0.28[b]
SAM combined (0.38)	SAM combined ICE 10% (0.57)	1.77[b]
SAM combined (0.38)	SAM combined ICE 20% (0.61)	2.11[b]
SAM combined (0.38)	SAM combined ICE 30% (0.69)	2.80[b]

[a] Critical value at 95% confidence interval is 1.96.
[b] Critical value at 95% confidence interval is 2.00.

Classification algorithms performed similarly, with MTMF classification (Table 2; MTMF/MNF/M) accuracies of 57% and 94% for producer's and user's accuracies, respectively, compared to SAM values (Table 2; SAM/MNF/M) of producer's and user's accuracies of 54% and 96%, respectively. Visual evaluation did not indicate a strong advantage to either algorithm, and statistical testing did not produce a significant difference between classifications (t-stat of 0.03; Table 3). We hypothesize that the similarities between classifications are due to a high degree of spectral distinctness of the mesic hoary cress endmember from background vegetation. For the remainder of this study, the SAM classification algorithm was used because it is easier than the MTMF algorithm to threshold consistently (lower degree of manual interpretation).

The accuracy resulting from using the xeric endmember (Table 2; SAM/MNF/X) is lower than the accuracy using the mesic endmember (Table 2; SAM/MNF/M). Although the accuracy from the xeric endmember is so low that Kappa is not significantly different from zero, the user's accuracy is high, and this classification outperformed the mesic endmember in xeric vegetative regimes, finding 17 additional infestations (Table 2; Fig. 2). Concatenation of the xeric and the mesic classifications into a single product (Table 2; SAM/MNF/C) generated higher producer's accuracy than either of the stand-alone endmembers (65%), at no cost to the user's accuracy. Further, Kappa testing demonstrated significantly greater accuracy using both the endmembers (combined) as compared to the accuracy of the xeric endmember alone (Table 3).

4.2. Post-processing

In addition to accuracy assessments, ICE analysis was used to determine the confidence in classifier performance and the detection limits for hoary cress. When applied to the mesic endmember (Table 2; SAM/MNF/M), ICE, with a 30% minimum cover threshold, yielded an increase in producer's accuracy from 54% to 64% (in comparison to using all percent covers). This increase was also associated with a high Kappa but a low t-statistic (Tables 2 and 3). A high Kappa value combined with an increase in producer's accuracy indicates that the classifier is working; however, the final accuracy (64%) is below acceptable limits for many management applications. Because previous processing methods documented a complimentary relationship between the xeric and mesic endmembers, it was hypothesized that the combination of these two would improve classification results. At a minimum of 30% hoary cress cover, the combined classifications increased producer's accuracy from 54% to 82%, with the same value of Kappa and a strong t-statistic (Tables 1 and 2). In this study, ICE analysis demonstrated that the addition of a second classification endmember significantly increased classifier performance, and since acceptable producers' and users' accuracies were determined at a reasonable hoary cress cover (82% accurate at greater than 30% cover), the classification is acceptable. Hoary cress infestations are detectable with cover as low as 10% (5 out of 19 positive validation samples at a cover between 0% and 10% were correctly identified). Confidence in the classification increased at 20% cover, but 30% hoary cress cover was necessary to produce accuracies useful for management applications.

4.3. Accuracy assessment

Design and implementation of representative field validation and accuracy assessment procedures are challenging and time-consuming portions of remote sensing studies, yet these procedures rarely receive adequate discussion (Aspinall, 2002). In this study, much of the area is privately owned by hundreds of different landowners. A well-developed network of roads accommodated spatially distributed samples. Some uncertainties in field validation were introduced as data was collected over two field seasons while hoary cress was in bloom (2003 and 2004). While collection of additional validation data a year after image acquisition is not ideal, it did provide the opportunity to augment the 2003 validation data. Field observations and discussions with local county weed managers and field crews indicated that significant changes to hoary cress cover in this time period were unlikely. Additionally, a sample size bias may exist for ICE analyses, because more positive validation samples were used to calculate accuracies at all percent covers of hoary cress than were used to calculate accuracies at minimum percent covers (Table 2).

Because there was a large georegistration error associated with the data, the accuracies presented are considered conservative. For example, the correct classification of some small infestations may not be accounted for due to the 25 m RMSE. This assumption was confirmed by repeating the accuracy assessment of the best prediction (SAM classified combined endmembers) when only considering large (>500 m^2) validation polygons, increasing producer's accuracy from 65% to 71% (for all percent covers). Calculated accuracies can be further complicated when comparing multiple classification products. As a result of these complications, it becomes necessary to evaluate accuracy beyond simple quantification of errors, using such techniques as ICE and qualitative analysis. Qualitative accuracy assessments are difficult to justify, yet play an integral role in map accuracy assessment. In this study, for example, confusion of hoary cress with windrows of recently harvested alfalfa was not captured in quantitative analysis due to a lack of validation data in that particular field. The concept is also illustrated by comparing the mesic and xeric endmembers. While the quantitative accuracies of the xeric endmember are low, the qualitative accuracy demonstrates that the classification is providing important information (Fig. 2).

4.4. Relevance to other studies

Ecological studies involving hyperspectral data require balanced consideration of project objectives with requirements for data collection and analysis (Aspinall et al., 2002). The techniques described herein can be used to enhance the understanding of data processing and the effects of permutations in hyperspectral image classification methodology. This study provides an example of hyperspectral image processing techniques in the context of vegetative discrimination with results satisfying management level needs. The use of multiple endmembers is likely applicable to many studies, especially in regions of variable topography or ecology. Additionally, the use of calculated accuracies has been demonstrated to be as much a tool in classification interpretation as it is representative of classification quality. Implementation of variable processing methods and innovative map interpretation techniques results in a deeper understanding of classifications and how they may be best utilized.

We conclude that the spectral distinctness of hoary cress allows for latitude between data transforms and classifiers; however, not all concepts presented in this study are directly portable to other projects attempting to discriminate hoary cress or similar vegetative species. Further, we hypothesize that high-resolution multispectral imagery may be able to discriminate high cover occurrences of hoary cress to accuracies approaching those presented in this study. However, further studies focusing on the necessary bandwidth for acceptable limits of hoary cress delineation are needed. We hypothesize that hyperspectral imagery is necessary to discriminate low percent cover hoary cress communities with confidence, such as 30% cover in a 3 m $\times$ 3 m pixel. Comparative results would be applicable if assessed using percent cover incremental analysis, such as presented herein.

Both the SAM and MTMF classification algorithms require the input of training endmembers, either in the form of regions of interest or spectral libraries, to classify a target. It is notable that, in this study, multiple endmembers were required for an optimal classification output. This represents a challenge to studies that wish to use hyperspectral data for management purposes. However, manuscripts such as presented herein (and other related work) combined with decreasing data costs will ultimately bridge the divide between technology and management needs.

5. Conclusions

This study successfully discriminated hoary cress in Ada County, Idaho, with producer's, user's, and overall accuracies of 82%, 79%, and 86%, respectively, for infestations with at least 30% cover. The most successful classification approach utilized MNF transformed reflectance data using two endmembers for hoary cress. In this study, the SAM (threshold of 1 radian) and MTMF (MF values greater than 0 and infeasibility values less than 15) comparison performed nearly identically (maximum 3% difference in accuracy). The MNF data transform outperformed the PCA rotation (23% higher producer's accuracy) in classification, demonstrating the utility of noise-whitening. The mesic endmember (producer's accuracy of 54%) outperformed the xeric endmember (producer's accuracy of 30%), but the combined endmember outperformed either of the parent classifications (producer's accuracy of 65%) while the user's accuracy remained high (95%). Removal of the low percent cover infestations increased the combined classification producer's accuracy to 82% while decreasing the user's accuracy to 79%. This study utilizes a sequential and quantitative methodology for hyperspectral vegetative discrimination output interpretation, which is applicable to other studies in similar environments.

Acknowledgements

This project was funded by the NASA BAA program (BAA-01-0ES-01; NAG13-02029). We thank Mr. William Graham of NASA Stennis for his continued support. Additional funding was contributed by the Idaho National Laboratory (INL) through the Idaho State University–INL Partnership for Integrated Environmental Analysis Education Outreach Program. The authors would like to acknowledge the Weed Control crews from Ada County and Bonneville County, Idaho, as well as Charlla Adams, Mark Strom and Ellen Wray-McComb from Boise State University for assistance with field data collection.

References

Aspinall, R. J. (2002). Use of logistic regression for validation of maps of the spatial distribution of vegetation species derived from high spatial resolution hyperspectral remotely sensed data. *Ecological Modeling 157*, 301–312.

Aspinall, R. J., Marcus, W. A., & Boardman, J. W. (2002). Considerations in collecting, processing, and analyzing high spatial resolution hyperspectral data for environmental investigations. *Journal of Geographic Systems 4*, 15–29.

Boardman, J. W. (1998). *Leveraging the high dimensionality of AVIRIS data for improved sub-pixel target unmixing and rejection of false positives: Mixture tuned matched filtering*. Proceedings of the 5th JPL Geoscience Workshop, Pasadena, CA.

Chen, D., & Stow, D. (2002). The effect of training strategies on supervised classification at different spatial resolutions. *Photogrammetric Engineering and Remote Sensing 68*(11), 1155–1161.

Congalton, R. G. (1991). A review of assessing the accuracy of classifications of remotely sensed data. *Remote Sensing of Environment* (37), 35–46.

Congalton, R. G., & Green, K. (1999). *Assessing the accuracy of remotely sensed data: Principles and practices*. Boca Raton: Lewis Publishers.

Davis, J. C. (1986). *Statistics and data analysis in geology*. (2nd edition). New York: John Wiley & Sons.

Everitt, J. H., Escobar, D. E., & Davis, M. R. (1995). Using remote sensing for detecting and mapping noxious plants. *Weed Abstracts 44*(12), 639–649.

Everitt, J. H., Escobar, D. E., & Davis, M. R. (2001). Reflectance and image characteristics of selected noxious rangeland species. *Journal of Range Management 54*, A106–A120.

Everitt, J. H., & Yang, C. (2004). Using Quickbird satellite imagery to distinguish two noxious weeds in southern Texas. *Proceedings of the 10th Forest Service Remote Sensing Conference*. Salt Lake City, UT: American Society of Photogrammetry and Remote Sensing.

Foody, G. M. (2002). Status of land cover classification accuracy assessment. *Remote Sensing of Environment 80*, 185–201.

Foody, G. M. (2004). Thematic map comparison: Evaluating the statistical significance of differences in classification accuracy. *Photogrammetric Engineering and Remote Sensing 70*(5), 627–633.

Gates, D. M., Keegan, H. J., Schleter, J. C., & Weidner, V. R. (1965). Spectral properties of plants. *Applied Optics 4*(1), 11–20.

Glenn, N. F., Mundt, J. T., Weber, K. T., Prather, T. S., Lass, L. W., & Pettingill, J. (2005). Hyperspectral data processing for repeat detection of small infestations of leafy spurge. *Remote Sensing of Environment 95*(3), 399–412.

Green, A. A., Berman, M., Switzer, P., & Craig, M. D. (1988). A transformation for ordering multispectral data in terms of image quality with implications for noise removal. *Transactions on Geoscience ad Remote Sensing 26*(1), 65–74.

Knipling, E. B. (1970). Physical and physiological basis for the reflectance of visible and near-infrared radiation from vegetation. *Remote Sensing of Environment 1*, 155–159.

Kondrat'yev, K. Y., & Fedchenko, P. P. (1981). Spectral reflectivity of weeds and useful plants. *Doklady Earth Science Sections 248*, 35–37.

Kruse, F. A., Boardman, J. W., Lefkoff, A. B., Young, J. M., & Kiereinn-Young, K. S. (2000). HyMap: An Australian hyperspectral sensor solving global problems—results from the USA HyMap data acquisitions. *Proceedings of the 10th Australian Remote Sensing and Photogrammetry Conference*. Adelaide, Australia: Casual Productions (CD-ROM).

Kruse, F. A., Lefkoff, A. B., Boardman, J. W., Heidebrecht, K. B., Shapio, A. T., Barloon, P. J., et al. (1993). The spectral image processing system (SIPS)—Interactive visualization and analysis of imaging spectrometer data. *Remote Sensing of Environment 44*, 145–163.

Lass, L. W., & Callihan, R. H. (1997). The effect of phenological stage on detectability of yellow hawkweed (*Hieracium partense*) and oxeye daisy (*Chrysanthemum leucanthemum*) with remote multispectral digital imagery. *Weed Technology 11*, 248–256.

Lillesand, T. M., & Kiefer, R. W. (2000). *Remote sensing and image interpretation*. (4th edition). New York: John Wiley & Sons.

Okin, W. J., Okin, G. S., Roberts, D. A., & Murray, B. (1998). *Multiple endmember spectral mixture analysis: Endmember choice in an arid shrubland*. Proceedings of the 5th AVIRIS Airborne Geosciences Workshop. JPL, CA.

Parker-Williams, A., & Hunt, E. R. (2002). Estimation of leafy spurge cover from hyperspectral imagery using Mixture Tuned Matched Filtering. *Remote Sensing of Environment 82*, 446–456.

Parker-Williams, A., & Hunt, E. R. (2004). Accuracy assessment for detection of leafy spurge with hyperspectral imagery. *Journal of Range Management 57*, 106–112.

Prather, T. S., Robins, S. S., Morishita, D. W., Lass, L. W., Callihan, R. H., & Miller, T. W. (2002). *Idaho's noxious weeds*. Moscow, ID: University of Idaho Press.

Roberts, D. A., Gardner, M., Church, R., Ustin, S. L., Scheer, G. J., & Green, R. O. (1998). Mapping chaparral in the Santa Monica Mountains using multiple endmember spectral mixture models. *Remote Sensing of Environment 65*, 267–279.

RSI. (2001). *ENVI FLAASH User's guide*. Boulder, CO: Research Systems, Inc.

Stehman, S. V. (1992). Comparison of systematic and random sampling for estimating the accuracy of maps generated from remotely sensed data. *Photogrammetric Engineering and Remote Sensing 58*(9), 1343–1350.

Stehman, S. V., & Czaplewski, R. L. (1998). Design and analysis for thematic map accuracy assessment: Fundamental principles. *Remote Sensing of Environment (64)*, 331–344.

Story, M., & Congalton, R. G. (1986). Accuracy assessment: A user's perspective. *Photogrammetric Engineering and Remote Sensing 52*(3), 397–399.

Underwood, E., Ustin, S. L., & DiPietro, D. (2003). Mapping nonnative plants using hyperspectral imagery. *Remote Sensing of Environment 86*, 150–161.